Journal of Physics and Chemistry of Solids xxx (2017) 1–5

Contents lists available at ScienceDirect

Journal of Physics and Chemistry of Solids

journal homepage: www.elsevier.com/locate/jpcs

Possible structural transformation and enhanced magnetic fluctuations in exfoliated α-$RuCl_3$

Boyi Zhou [a], Yiping Wang [b], Gavin B. Osterhoudt [b], Paula Lampen-Kelley [c], David Mandrus [d,c], Rui He [e], Kenneth S. Burch [b], Erik A. Henriksen [a,f,*]

[a] Department of Physics, Washington University in St. Louis, 1 Brookings Dr., St. Louis, MO 63130, USA
[b] Boston College Department of Physics, 140 Commonwealth Avenue, Chestnut Hill, MA 02467, USA
[c] Material Science & Technology Division, Oak Ridge National Laboratory, Oak Ridge, TN 37831, USA
[d] Department of Material Science and Engineering, University of Tennessee, Knoxville, TN 37996, USA
[e] Department of Electrical and Computer Engineering, Texas Tech University, Lubbock, TX 79409, USA
[f] Institute for Materials Science & Engineering, Washington University in St. Louis, 1 Brookings Dr., St. Louis, MO 63130, USA

ARTICLE INFO

Keywords:
A. Magnetic materials
C. Raman spectroscopy
D. Phonons

ABSTRACT

We present Raman spectroscopy experiments on exfoliated α-$RuCl_3$, from tens of nm thick down to single layers. Besides unexpectedly finding this material to be air stable, in the thinnest layers we observe the appearance with decreasing temperature of a symmetry-forbidden mode in crossed polarization, along with an anomalous broadening of a mode at 164 cm^{-1} that is known to couple to a continuum of magnetic excitations. This may be due to an enhancement of magnetic fluctuations and evidence for a distorted honeycomb lattice in single- and bilayer samples.

1. Introduction

Just over a decade ago, Kitaev proposed a model of a many-body ground state that can be exactly solved, yielding a spin liquid with Majorana Fermion excitations [1,2]. He considered a honeycomb lattice with spin 1/2 moments experiencing a bond-dependent exchange, such that different components of the spin couple along different bonds (see Fig. 1a). This model can be realized in materials under the right conditions of crystal electric field, spin-orbit coupling and on-site Coulomb repulsion that produce an insulator with $J_{eff} = 1/2$ moments. In systems where the honeycomb lattice is formed by placing the magnetic atom inside edge-sharing octahedra, one can realize the necessary bond-dependent exchange due to the impact of strong spin-orbit coupling on the hopping (see Fig. 1) [3–6]. A key difficulty with this proposal is that additional interaction terms may arise and produce long range order [7–10]. While some of these terms are enabled simply by symmetry, they are strongly enhanced by lattice distortions that mix the $J_{eff} = 1/2$ and $J_{eff} = 3/2$ states, altering the hopping terms.

Recently, α-$RuCl_3$ has emerged as a potential candidate to realize a Kitaev quantum spin liquid state [2,11–21]. IR, Raman and photo-emission spectroscopy combined with DFT calculations strongly suggest the system is close to the $J_{eff} = 1/2$ limit, with octahedra that are nearly undistorted at low temperatures. Perhaps due to the smaller spin-orbit coupling expected in a 4*d* system, α-$RuCl_3$ reveals an extremely narrow spin-orbit exciton (2 meV wide) well separated from charge excitations [15]. Thus the low-energy model of α-$RuCl_3$ does not contain any charge fluctuations, unlike the 5*d* Ir systems where the spin-orbit and onsite $d-d$ excitations are overlapped in energy [10]. Perhaps most promising is the observed continuum of magnetic excitations, where the Raman temperature dependence and the excitation dispersion seen by neutrons is consistent with fractional particles expected from the pure Kitaev model [2,12,14,21,22].

Despite its importance to the formation of an ordered state, the structure of α-$RuCl_3$ remains controversial. In particular, the exact structure appears to be sensitive to atomic disorder and stacking faults, which are not uncommon in van der Waals crystals [16,22,23]. Surprisingly, the addition of stacking faults leads to an enhanced onset of antiferromagnetic order (higher $T_{Néel}$) [16]. This rather counterintuitive observation may result from additional hopping pathways opened by the stacking disorder that strengthen the Heisenberg terms. If correct, this suggests that exfoliating α-$RuCl_3$ down to single layers could suppress the long range order and perhaps stabilize the quantum spin liquid.

Through the use of applied magnetic fields, a number of probes now suggest that once the long range magnetic order is suppressed, a spin

* Corresponding author. Department of Physics, Washington University in St. Louis, 1 Brookings Dr., St. Louis, MO 63130, USA.
E-mail address: henriksen@wustl.edu (E.A. Henriksen).

https://doi.org/10.1016/j.jpcs.2018.01.026
Received 24 August 2017; Received in revised form 7 December 2017; Accepted 14 January 2018
Available online xxxx
0022-3697/

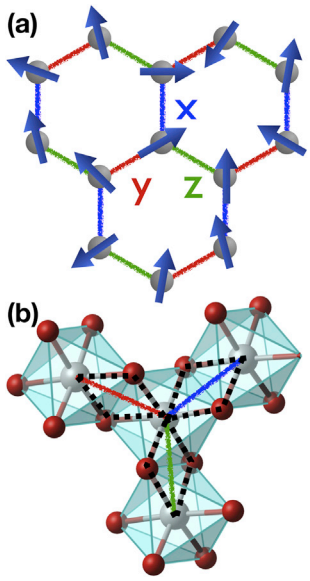

Fig. 1. (a) Kitaev model of spin 1/2 on the honeycomb lattice with the three in-equivalent bonds indicated by the interacting component of the spin. (b) Structure of the ideal α-$RuCl_3$ lattice, with Cl atoms octahedrally coordinated around each Ru. The hopping pathways are indicated by black dashed lines, which for a perfect $J_{eff} = 1/2$ state will lead to a Kitaev interaction.

liquid state emerges [8,20,24–27]. If a similar suppression can be achieved through exfoliation to few or single-layer thick crystals, the resulting state could be closer to the original Kitaev proposal. In addition, exfoliated α-$RuCl_3$ would allow one to bring many well-developed techniques for exploring 2D atomic crystals to bear, for instance by utilizing van der Waals heterostructures to control the local environment and perhaps even exploit proximity effects [28,29]. Crucial to this approach will be the evolution of the lattice and electronic structure that ultimately control the balance between the various exchange terms. Inelastic light scattering provides an excellent means to explore these issues. Raman has already demonstrated its utility in determining the lattice structure, symmetry, magnetic order, two-magnon excitations, magneto-elastic coupling, and disorder in various 2D materials [30–34]. In α-$RuCl_3$, bulk measurements have revealed how magnetic fluctuations interact with the lattice via an asymmetric phonon broadening (i.e. Fano lineshapes) [12]. Further, Raman experiments have shown hysteresis of a structural transition along with associated changes in the spectrum of magnetic excitations [22].

To directly address the possibility of tuning the behavior of α-$RuCl_3$ via exfoliation, we have studied the Raman spectra of exfoliated crystals with thicknesses ranging from 43 nm down to single layers less than 1 nm thick. We have measured the polarization and temperature dependence from room temperature to 10 K. While the thicker pieces produce spectra similar to those seen in bulk, in thin layers we observe an anomalous broadening of the phonons with temperature. Particular attention is paid to a mode already shown to exhibit strong coupling to the magnetic excitations, suggesting an enhanced broadening from additional magnetic fluctuations in thin layers. Intriguingly, we also find an A_{1g} phonon mode—forbidden by symmetry to appear in crossed polarization—is nonetheless observed in the thinnest samples at low temperatures. This is suggestive of a structural transition driven by the decreasing thickness or by strain incurred in the process of exfoliation.

2. Exfoliation

Single crystal α-$RuCl_3$ samples were grown using a vapor transport technique from phase pure commercial $RuCl_3$ powder [21]. These bulk crystals were mechanically exfoliated onto Si/SiO_2 substrates using scotch tape following the methods used for graphene and other van der Waals materials [35]. Exfoliation yielded monolayer, bilayer and multilayer flakes with typical sizes of $10 - 30\ \mu m$, which were first identified by optical color contrast (Fig. 2a). The thicknesses were then checked by atomic force microscopy (Fig. 2b). Typical single layer thicknesses were 0.8 nm, thicker than the ≈ 0.6 nm found by xray diffraction [16]; such height discrepancies have been previously noticed in α-$RuCl_3$ and other layered materials and attributed to incidental water adsorption [36,37]. Fortuitously, α-$RuCl_3$ appears to be stable in air: we find the Raman spectra of all thicknesses even down to monolayers to be reproducible after months of exposure to air, even after transportation between separate labs for repeated measurements (see Fig. 2c).

3. Raman

Raman spectroscopy was performed on monolayer, bilayer and multilayer α-$RuCl_3$ samples on Si/SiO2 over a range of temperatures. Room temperature spectra were measured in air in a Raman spectrometer with a 514 nm excitation laser and low energy cut-off of 100 cm^{-1}. The laser spot size was $\approx 2\ \mu m$ with a resolution of 1.8 cm^{-1}. Low temperature measurements were performed separately under vacuum in a cryostat down to 10 K. These measurements were made in the quasi-backscattering geometry in crossed (XY) polarization, with light polarized in the basal (cleavage) plane. Light from a 532 nm laser was focused down to a 2 μm spot with an estimated power of 160 μW. The resolution of the low temperature Raman system was 2 cm^{-1}. To confirm heating was not a contributing factor to the additional broadening, additional experiments were performed in a custom-built low temperature Raman setup where the anti-Stokes spectra could be collected [38]. The ratio of the Stokes to anti-Stokes intensity confirmed the excitation power used did not lead to significant heating ($\Delta T \leq 10$ K). We work in back-scattering geometry described by the Porto notation $c(IS)\bar{c}$, where c

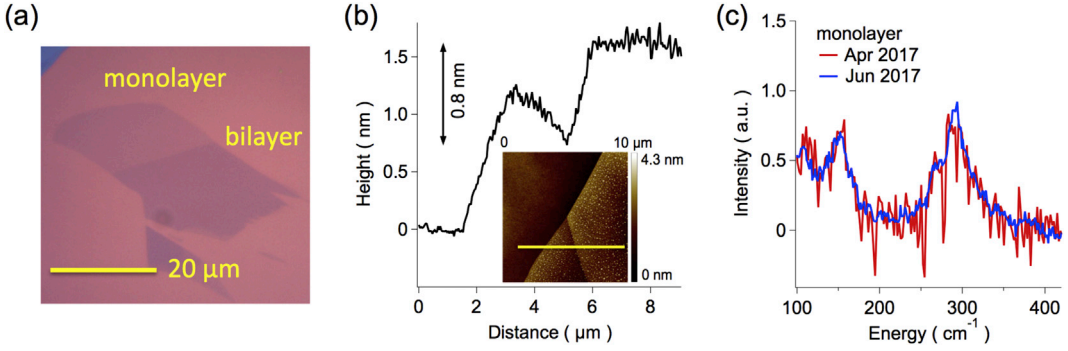

Fig. 2. Exfoliated α-$RuCl_3$. (a) Optical image showing contrast of mono and bilayer flake. (b) Atomic force microscope image of same flake. (c) Air stability of monolayer α-$RuCl_3$ as demonstrated by Raman spectroscopy: the red and blue traces were acquired in separate measurements made 2.5 months apart in different cryostats. (For interpretation of the references to color in this figure legend, the reader is referred to the Web version of this article.)

refers to propagation of the light along the *c*-axis, and *I* (*S*) is the axis along which the incident (scattered) light is polarized.

In measurements of multilayer stacks of thin-films, Fabry-Perot interference can result in strong deviations of the Raman intensity [30, 39–43], though we note these are unlikely to be strongly temperature dependent. Multiple reflections of both the incident excitation laser and of the Raman scattered light can occur due to the multiple interfaces present. If the optical constants of the constituent materials are known, it is possible to compute the net effect this has on the spectra and then normalize it out. The computation consists of two parts. First, the enhancements of the incident and scattered light at a given depth of the material are calculated. Then, these two enhancements are multiplied and integrated over the thickness of the sample to obtain a total enhancement factor. Applying this procedure to our data, each Raman spectrum is divided by the final enhancement factor, after a detector-dependent dark count was subtracted [43,44].

4. Thickness and temperature dependence

We begin with the thickness dependence of the Raman spectra of α-$RuCl_3$ at high and low temperatures. In Fig. 3a we show the thickness dependence of the unpolarized Raman spectra at room temperature, revealing both a nearly three order-of-magnitude decrease in the Raman response with reduced thickness, along with a notable increase in the broadening of all phonon modes for flakes thinner than ≈ 6 nm. As the broadening increases the three individual phonon peaks in the group between 270 and 315 cm^{-1} merge. Fits to this data nonetheless give the best results when three Lorentzians are used over this range for all thicknesses, suggesting the individual modes still exist in the thinnest flakes. The source of this broadening is not immediately clear, but its occurrence in only the thinnest flakes suggests it may be related to the exfoliation process. For instance, prior work in graphene has demonstrated that exfoliated flakes show a range of residual strain [45] that may, in the present system, distort the lattice sufficiently to broaden the modes. In lieu of such global strain, the ~nm-scale roughness of the supporting SiO_2 may induce a locally varying strain potential impacting thinner flakes more due to their reduced stiffness. We note that two weaker modes at 116 cm^{-1} and 220 cm^{-1} appear to vanish in the thinnest flakes but may simply have become too broad to be distinguished from the noise. In short, beyond the loss of intensity with reduced thickness, and the increased broadening, there is little change from the known spectra of bulk α-$RuCl_3$ [12,22].

In contrast, the thickness dependence at low temperature shows an interesting anomaly (see Fig. 3b). In XY polarization, thicker flakes reveal only two strong peaks near 270 and 300 cm^{-1} (marked by downward arrows), in agreement with the previous results of Ref. [12] for Raman of bulk α-$RuCl_3$. There the authors invoked weak interlayer coupling to adopt a D_{3d} symmetry for single layers, which in contrast to the $C2/m$ monoclinic structure reported by x-ray diffraction [13,16] correctly predicts the observed polarization dependence: namely that phonon modes of both A and E symmetry are seen in colinear XX polarization but only E modes appear in crossed XY polarization. However, in the thinnest samples in Fig. 3(b), the symmetry-forbidden A mode unexpectedly appears as a robust third peak at 315 cm^{-1}. A weak signal at 315 cm^{-1} is seen in the 23.8 nm flake at 10 K, but this is likely due to polarizer mis-alignment.

To investigate the appearance of this symmetry-forbidden mode, we measured the temperature dependence of the Raman spectra in three samples: a 'bulk' flake 23.8 nm thick, along with bilayer and monolayer flakes. These data, acquired in XY configuration, are shown in Fig. 4, where we immediately observe a strong difference in the response of the bilayer and single layer compared to the thicker flake. Similar to previous bulk measurements performed in XY geometry, the 23.8 nm sample primarily reveals modes of E_g symmetry at all temperatures [12], all of which strengthen with decreasing temperature. The most pronounced effect seen occurs in the mode at 164 cm^{-1}, which acquires a significant Fano lineshape at low temperatures but does not reveal strong broadening with increased temperature. In contrast, in the thinnest layers (Fig. 4b,c), the symmetry-forbidden mode at 315 cm^{-1} is clearly observed at low temperatures. Moreover, this mode exhibits a curiously strong temperature dependence: while all phonons peaks are observed to sharpen with decreasing temperature, this 315 cm^{-1} phonon is barely visible at all at room temperature, but rapidly grows in intensity as the temperature is lowered. The similar behavior of the mono- and bilayer flakes confirms this behavior is not an isolated event. Additionally, the mode at 164 cm^{-1} in the thin samples undergoes a strong increase in width with temperature.

Applying Lorentzian fits to quantify the temperature dependence of these peaks, we find the lower signal-to-noise in the thinner samples leads to large error bars in the intensity and width of the modes between 270 and 315 cm^{-1}. Therefore we turn our attention to the more visible phonon mode at 164 cm^{-1}, which we note has been established to strongly couple to the magnetic fluctuations [12]. In measurements of bulk crystals, this mode acquires a Fano lineshape ascribed to interactions with a continuum of magnetic excitations, and indeed a Fano lineshape is clearly visible in our data (see Fig. 4). We performed Fano fits to the data in a limited range around this peak. The results for the frequency and linewidth for five different thicknesses are shown in Fig. 5. For samples thicker than bilayers we find behavior consistent with the bulk results, namely a small softening resulting from anharmonicity [46], and a broadening above 100 K attributed to standard phonon decay into two acoustic modes [47]. The divergence of the mono- and bilayer samples' behavior from that of the thicker material is rather striking. While at the lowest temperatures both the central energies and widths are closely matched for all samples, as the temperature increases the mono- and bilayer data diverge, revealing a much stronger mode softening accompanied by a sharp increase of the width, which at room temperature is $2-3$ times broader than the same mode in thicker samples.

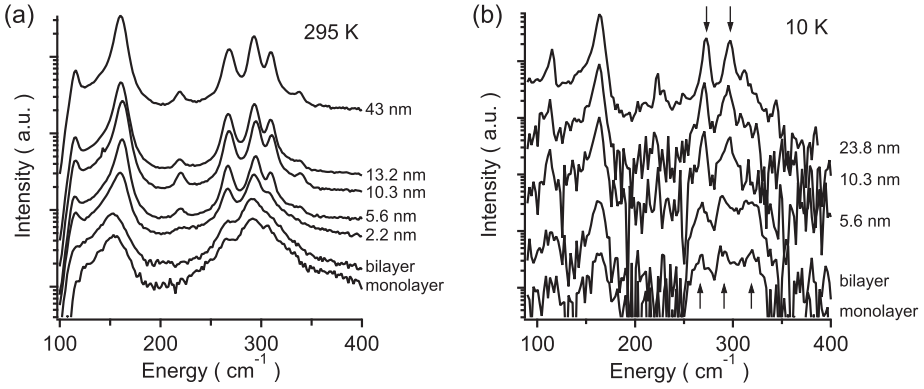

Fig. 3. Thickness dependence of Raman measurements: (a) unpolarized spectra at room temperature, and (b) in XY polarization at low temperature. Plots are shown as log intensity due to the large signal decrease with thickness. Traces in (b) are vertically offset for clarity; no offsets are applied in (a).

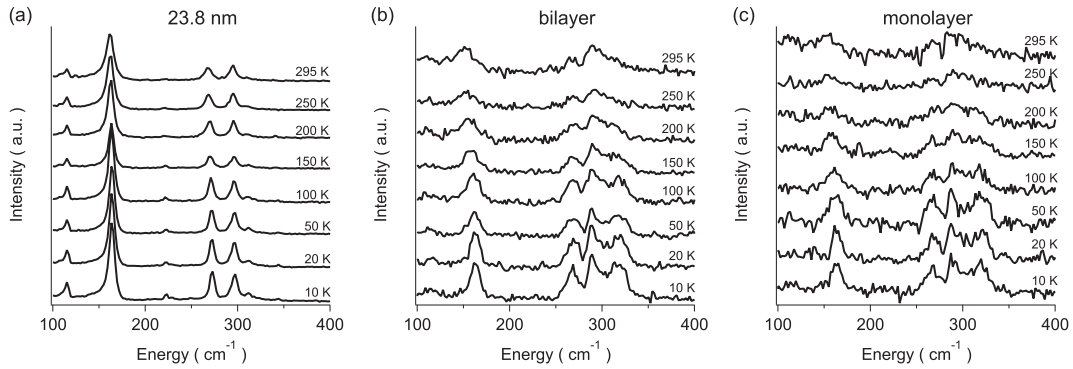

Fig. 4. Temperature dependence of Raman spectra for various thickness flakes, measured in XY polarization: (a) bulk exfoliated crystal, 23.8 nm thick; (b) bilayer; and (c) monolayer.

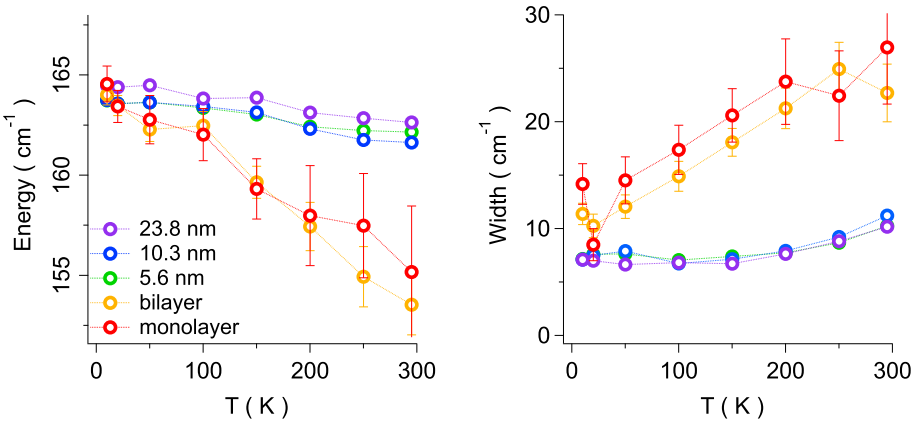

Fig. 5. Temperature dependence of the (a) energy and (b) width of the 164 cm^{-1} phonon (labeled by its energy at low temperature), for five different flake thicknesses.

5. Discussion

The robust appearance of the 315 cm^{-1} mode in XY scattering is surprising. Undistorted layers with D_{3d} symmetry should contain both the E_g and A_{1g} modes, with the A_{1g} mode disappearing in the XY configuration. As noted, this was seen in bulk material in Ref. [12], and found to be consistent with the behavior observed for the magnetic continuum. Here the thicker flakes show the expected two modes at 270 and 300 cm^{-1} to dominate in XY scattering although we note the nominally forbidden mode does appear, albeit with a very low intensity. This suggests the onset of a small distortion of the lattice that becomes strongest in the thinnest flakes. However, perhaps the A mode appears in all samples due to simple polarizer mis-alignment. Yet if that were true, i) the observed strong temperature dependence would not be expected, and ii) the mode should appear in the thicker flake with more or less the same relative intensity as in the thinner flakes, but this is not observed.

Thus overall we find the two thinnest samples stand out by the appearance of a symmetry-forbidden mode and an unusual behavior of the lower energy, Fano-shaped mode. Is a common cause behind these observations? Structural disorder is an obvious culprit: as mentioned, thin flakes exfoliated on Si/SiO_2 can have a range of built-in tension [45], which here may introduce distortions of the Cl octahedra and enable otherwise forbidden phonons to appear. Moreover stacking faults are readily introduced into α-$RuCl_3$ by bending [16], and the mechanical exfoliation process is surely not gentle. Yet the thicker, bulk-like flakes provide little evidence for the mode in XY. Combined with our observation that at low temperatures the energies and linewidths of all modes are very close to that of bulk samples, we rule out any major structural reorganization. Instead, our results suggest a strong distortion appears only in the thinnest layers.

On the other hand, the 164 cm^{-1} phonon width may be broadened by a variety of physical mechanisms: disorder, an increase in anharmonic phonon scattering, and especially magnetic fluctuations which are already known to drive the Fano lineshape. Examining Fig. 5, we see at the lowest temperatures both the central energy and the linewidth values closely agree across all samples at the lowest temperatures. Since static disorder will dominate as $T \rightarrow 0$, it would appear that the disorder potential in the thinnest flakes is not significantly stronger than that affecting the thicker ones. Thus we may contemplate more exotic origins of the distortion, for instance, the possibility of a strong magneto-elastic coupling generating a distortion in order to stabilize magnetic order, driven by the large entropy of the proximate quantum spin liquid. Nonetheless, the strong temperature dependence of the linewidth suggests enhanced magnetic fluctuations may be the cause of the strong broadening in thin layers.

6. Conclusion

In this paper we explored the possibility of destroying the long range order in α-$RuCl_3$ by exfoliating down to a single monolayer. The Raman spectra are consistent with the overall structure remaining intact, however the appearance of a mode in both XX and XY configurations suggest the development of significant in-plane distortions away from the perfect honeycomb lattice. If correct this suggests enhancement of non-Kitaev terms in the exchange that could further stabilize the ordered state. At the moment the origin of this distortion is unclear. The exfoliation process, or the use of non-flat substrates, may contribute significant strain leading to the distorted structure, but further Raman and x-ray studies on various substrates [48] will be required to clarify both the structure, and the role played by the substrate. We also note that the phonons in mono- and bilayer samples reveal significant additional temperature dependence. This could result from the additional distortion leading to

enhanced anharmonicity. However a much more intriguing possibility is that enhanced magnetic fluctuations in thin layers strongly reduces the lifetime of the phonons. Studies on substrates with reduced background contributions and further enhancements of the Raman via interference would enable closer examination of the magnetic fluctuations. Nonetheless our results clearly demonstrate the possibility of tuning the Kitaev paramagnetic state in α-$RuCl_3$ via exfoliation.

Acknowledgements

Work at Boston College was completed with support from the National Science Foundation (grant DMR-1709987). BZ and EAH acknowledge support from the Institute of Materials Science & Engineering at Washington University in St. Louis. RH acknowledges support by the National Science Foundation CAREER Grant (No. DMR- 1760668). P.L.K and D.M. were supported by the Gordon and Betty Moore Foundation EPiQS Initiative Grant GBMF4416. We are grateful to J. Knolle, T. Berlijn, and N. Perkins for fruitful discussions.

References

[1] A.Y. Kitaev, Anyons in an exactly solved model and beyond, Ann. Phys. 321 (1) (2006) 2–111.
[2] J. Nasu, J. Knolle, D.L. Kovrizhin, Y. Motome, R. Moessner, Fermionic response from fractionalization in an insulating two-dimensional magnet, Nat. Phys. 12 (10) (2016) 912–915.
[3] G. Jackeli, G. Khaliullin, Mott insulators in the strong spin-orbit coupling limit: from Heisenberg to a quantum compass and Kitaev models, Phys. Rev. Lett. 102 (1) (2009) 017205.
[4] J. Chaloupka, G. Jackeli, G. Khaliullin, Kitaev-heisenberg model on a honeycomb lattice: possible exotic phases in iridium oxides $A2_IrO_3$, Phys. Rev. Lett. 105 (2) (2010) 027204.
[5] B.J. Kim, H. Jin, S.J. Moon, J.Y. Kim, B.G. Park, C.S. Leem, J. Yu, T.W. Noh, C. Kim, S.J. Oh, J.H. Park, V. Durairaj, G. Cao, E. Rotenberg, Novel J_{eff}=1/2 Mott state induced by relativistic spin-orbit coupling in Sr_2IrO_4, Phys. Rev. Lett. 101 (7) (2008) 076402–076404.
[6] A. Catuneanu, Y. Yamaji, G. Wachtel, H.-Y. Kee, Y.B. Kim, Realizing Quantum Spin Liquid Phases in Spin-orbit Driven Correlated Materials, arXiv.org/cond-mat, 2017, p. 1701, 07837.
[7] H.-S. Kim, V.S.V.,A. Catuneanu, H.-Y. Kee, Kitaev magnetism in honeycomb $RuCl_3$ with intermediate spin-orbit coupling, Phys. Rev. B 91 (24) (2015) 241110.
[8] R. Yadav, N.A. Bogdanov, V.M. Katukuri, S. Nishimoto, J. van den Brink, L. Hozoi, Kitaev exchange and field-induced quantum spin-liquid states in honeycomb α-RuCl3, Sci. Rep. 6 (2016) 37925.
[9] I.I. Mazin, H.O. Jeschke, K. Foyevtsova, R. Valentí, D.I. Khomskii, Na_2IrO_3 as a molecular orbital crystal, Phys. Rev. Lett. 109 (19) (2012) 197201–197205.
[10] H. Gretarsson, J.P. Clancy, X. Liu, J.P. Hill, E. Bozin, Y. Singh, S. Manni, P. Gegenwart, J. Kim, A.H. Said, D. Casa, T. Gog, M.H. Upton, H.-S. Kim, J. Yu, V.M. Katukuri, L. Hozoi, J. van den Brink, Y.-J. Kim, Crystal-field splitting and correlation effect on the electronic structure of A_2IrO_3, Phys. Rev. Lett. 110 (7) (2013) 076402–076405.
[11] K.W. Plumb, J.P. Clancy, L.J. Sandilands, V.V. Shankar, Y.F. Hu, K.S. Burch, H.-Y. Kee, Y.-J. Kim, α-$RuCl_3$: a spin-orbit assisted Mott insulator on a honeycomb lattice, Phys. Rev. B 90 (4) (2014) 041112.
[12] L.J. Sandilands, Y. Tian, K.W. Plumb, Y.-J. Kim, K.S. Burch, Scattering continuum and possible fractionalized excitations in α-$RuCl_3$, Phys. Rev. Lett. 114 (14) (2015) 147201.
[13] R.D. Johnson, S.C. Williams, A.A. Haghighirad, J. Singleton, V. Zapf, P. Manuel, I.I. Mazin, Y. Li, H.O. Jeschke, R. Valent, R. Coldea, Monoclinic crystal structure of α-$RuCl_3$ and the zigzag antiferromagnetic ground state, Phys. Rev. B 92 (23) (2015) 235119.
[14] A. Banerjee, C.A. Bridges, J.Q. Yan, A.A. Aczel, L. Li, M.B. Stone, G.E. Granroth, M.D. Lumsden, Y. Yiu, J. Knolle, S. Bhattacharjee, D.L. Kovrizhin, R. Moessner, D.A. Tennant, D.G. Mandrus, S.E. Nagler, Proximate Kitaev quantum spin liquid behaviour in a honeycomb magnet, Nat. Mater. 15 (7) (2016) 733–740.
[15] L.J. Sandilands, Y. Tian, A.A. Reijnders, H.-S. Kim, K.W. Plumb, Y.-J. Kim, H.-Y. Kee, K.S. Burch, Spin-orbit excitations and electronic structure of the putative Kitaev magnet α-$RuCl_3$, Phys. Rev. B 93 (7) (2016) 075144.
[16] H.B. Cao, A. Banerjee, J.Q. Yan, C.A. Bridges, M.D. Lumsden, D.G. Mandrus, D.A. Tennant, B.C. Chakoumakos, S.E. Nagler, Low-temperature crystal and magnetic structure of α-$RuCl_3$, Phys. Rev. B 93 (13) (2016) 134423.
[17] Y. Kubota, H. Tanaka, T. Ono, Y. Narumi, K. Kindo, Successive magnetic phase transitions in α-$RuCl_3$: XY-like frustrated magnet on the honeycomb lattice, Phys. Rev. B 91 (9) (2015) 094422.
[18] F. Lang, P.J. Baker, A.A. Haghighirad, Y. Li, D. Prabhakaran, R. Valentí, S.J. Blundell, Unconventional magnetism on a honeycomb lattice in α-$RuCl_3$ studied by muon spin rotation, Phys. Rev. B 94 (2) (2016) 020407.
[19] X. Zhou, H. Li, J.A. Waugh, S. Parham, H.-S. Kim, J.A. Sears, A. Gomes, H.-Y. Kee, Y.-J. Kim, D.S. Dessau, Angle-resolved photoemission study of the Kitaev candidate α-$RuCl_3$, Phys. Rev. B 94 (16) (2016) 161106.
[20] K. Ran, J. Wang, W. Wang, Z.-Y. Dong, X. Ren, S. Bao, S. Li, Z. Ma, Y. Gan, Y. Zhang, J.T. Park, G. Deng, S. Danilkin, S.-L. Yu, J.-X. Li, J. Wen, Spin-wave excitations evidencing the Kitaev interaction in single crystalline α-$RuCl_3$, Phys. Rev. Lett. 118 (2017) 107203.
[21] A. Banerjee, J. Yan, J. Knolle, C.A. Bridges, M.B. Stone, M.D. Lumsden, D.G. Mandrus, D.A. Tennant, R. Moessner, S.E. Nagler, Neutron scattering in the proximate quantum spin liquid α-$RuCl_3$, Science 356 (6342) (2017) 1055–1059.
[22] A. Glamazda, P. Lemmens, S.H. Do, Y.S. Kwon, K.Y. Choi, Relation between Kitaev magnetism and structure in α-$RuCl_3$, Phys. Rev. B 95 (2017) 174429.
[23] M. Ziatdinov, A. Banerjee, A. Maksov, T. Berlijn, W. Zhou, H.B. Cao, J.Q. Yan, C.A. Bridges, D.G. Mandrus, S.E. Nagler, A.P. Baddorf, S.V. Kalinin, Atomic-scale observation of structural and electronic orders in the layered compound α-$RuCl_3$, Nat. Commun. 7 (2016) 13774.
[24] I.A. Leahy, C.A. Pocs, P.E. Siegfried, D. Graf, S.H. Do, K.-Y. Choi, B. Normand, M. Lee, Anomalous thermal conductivity and magnetic torque response in the honeycomb magnet α-$RuCl_3$, Phys. Rev. Lett. 118 (2017) 187203.
[25] J.A. Sears, Y. Zhao, Z. Xu, J.W. Lynn, Y.-J. Kim, Phase diagram of α-$RuCl_3$ in an in-plane magnetic field, Phys. Rev. B 95 (18) (2017) 180411–180415.
[26] D. Hirobe, M. Sato, Y. Shiomi, H. Tanaka, E. Saitoh, Magnetic thermal conductivity far above the Néel temperature in the Kitaev-magnet candidate α-$RuCl_3$, Phys. Rev. B 95 (24) (2017) 241112–241116.
[27] A.U.B. Wolter, L.T. Corredor, L. Janssen, K. Nenkov, S. Schönecker, S.H. Do, K.Y. Choi, R. Albrecht, J. Hunger, T. Doert, M. Vojta, B. Büchner, Field-induced quantum criticality in the Kitaev system α-$RuCl_3$, Phys. Rev. B 96 (4) (2017) 609–615.
[28] A.K. Geim, I.V. Grigorieva, Van der Waals heterostructures, Nature 499 (7459) (2013) 419–425.
[29] D. Jariwala, T.J. Marks, M.C. Hersam, Mixed-dimensional van der Waals heterostructures, Nat. Mater. 16 (2) (2016) 170–181.
[30] L.J. Sandilands, J.X. Shen, G.M. Chugunov, S.Y.F. Zhao, S. Ono, Y. Ando, K.S. Burch, Stability of exfoliated $Bi_2Sr_2Dy_xCa_{1-x}Cu_2O_{8+\delta}$ studied by Raman microscopy, Phys. Rev. B 82 (2010) 064503.
[31] A.C. Ferrari, D.M. Basko, Raman spectroscopy as a versatile tool for studying the properties of graphene, Nat. Nanotechnol. 8 (4) (2013) 235–246.
[32] Y. Tian, M.J. Gray, H. Ji, R.J. Cava, K.S. Burch, Magneto-elastic coupling in a potential ferromagnetic 2D atomic crystal, 2D Mater. 3 (2017) 025035.
[33] L. Wang, I. Gutiérrez-Lezama, C. Barreteau, D.-K. Ki, E. Giannini, A.F. Morpurgo, Direct observation of a long-range field effect from gate tuning of nonlocal conductivity, Phys. Rev. Lett. 117 (17) (2016) 176601–176606.
[34] J.-U. Lee, S. Lee, J.H. Ryoo, S. Kang, T.Y. Kim, P. Kim, C.-H. Park, J.-G. Park, H. Cheong, Ising-type magnetic ordering in atomically thin $FePS_3$, Nano Lett. 16 (12) (2016) 7433.
[35] K.S. Novoselov, D. Jiang, F. Schedin, T.J. Booth, V.V. Khotkevich, S.V. Morozov, A.K. Geim, Two-dimensional atomic crystals, Proc. Natl. Acad. Sci. Unit. States Am. 102 (30) (2005) 10451.
[36] D. Weber, L.M. Schoop, V. Duppel, J.M. Lippmann, J. Nuss, B.V. Lotsch, Magnetic properties of restacked 2D spin 1/2 honeycomb $RuCl_3$ nanosheets, Nano Lett. 16 (6) (2016) 3578–3584.
[37] K. Nagashio, T. Yamashita, T. Nishimura, K. Kita, A. Toriumi, Electrical transport properties of graphene on SiO_2 with specific surface structures, J. Appl. Phys. 110 (2) (2011) 024513.
[38] Y. Tian, A.A. Reijnders, G.B. Osterhoudt, I. Valmianski, J.G. Ramirez, C. Urban, R. Zhong, J. Schneeloch, G. Gu, I. Henslee, K.S. Burch, Low vibration high numerical aperture automated variable temperature Raman microscope, Rev. Sci. Instrum. 87 (4) (2016) 043105.
[39] R.J. Nemanich, C.C. Tsai, G.A.N. Connell, Interference-enhanced Raman scattering of very thin titanium and titanium oxide films, Phys. Rev. Lett. 44 (4) (1980) 273–276.
[40] M. Ramsteiner, C. Wild, J. Wagner, Interference effects in the Raman scattering intensity from thin films, Appl. Optic. 28 (18) (1989) 4017–4023.
[41] P. Blake, A.H. Castro Neto, K.S. Novoselov, D. Jiang, R. Yang, A.K. Geim, Making graphene visible, Appl. Phys. Lett. 91 (6) (2007) 063124.
[42] H. Zhang, Y. Wan, Y. Ma, W. Wang, Y. Wang, L. Dai, Interference effect on optical signals of monolayer MoS_2, Appl. Phys. Lett. 107 (10) (2015), 101904–4.
[43] S.Y.F. Zhao, C. Beekman, L.J. Sandilands, J.E.J. Bashucky, D. Kwok, N. Lee, A.D. LaForge, S.W. Cheong, K.S. Burch, Fabrication and characterization of topological insulator Bi_2Se_3 nanocrystals, Appl. Phys. Lett. 98 (14) (2011) 141911.
[44] D. Yoon, H. Moon, Y.-W. Son, J.S. Choi, B.H. Park, Y.H. Cha, Y.D. Kim, H. Cheong, Interference effect on Raman spectrum of graphene on SiO_2/Si, Phys. Rev. B 80 (12) (2009) 125422.
[45] J.S. Bunch, A.M. Van Der Zande, S. Verbridge, I. Frank, D. Tanenbaum, J.M. Parpia, H.G. Craighead, P.L. McEuen, Electromechanical resonators from graphene sheets, Science 315 (5811) (2007) 490.
[46] R.P. Lowndes, Anharmonicity in the silver and thallium halides: far-infrared dielectric response, Phys. Rev. B 6 (4) (1972) 1490–1498.
[47] P.G. Klemens, Anharmonic decay of optical phonons, Phys. Rev. 148 (2) (1966) 845–848.
[48] A. Lupascu, R. Feng, L.J. Sandilands, Z. Nie, V. Baydina, G. Gu, S. Ono, Y. Ando, D.C. Kwok, N. Lee, S.W. Cheong, K.S. Burch, Y.-J. Kim, Structural study of $Bi_{[2]}Sr_{[2]}CaCu_{[2]}O_{8+\delta}$ exfoliated nanocrystals, Appl. Phys. Lett. 101 (22) (2012) 223106.